

# EDGE-ENRICHED SULFUR-DOPED POROUS CARBON NANOFLEAKS FOR OXYGEN REDUCTION REACTION IN ZINC-AIR BATTERY

Yiyi She<sup>1</sup>, An Wang<sup>2</sup>, Jin Liu<sup>1</sup>, Jinsong Zhou<sup>1</sup>, Li Li<sup>3</sup>, Hongkang Wang<sup>2</sup>, Michael K.H. Leung<sup>1\*</sup>

<sup>1</sup>Ability R&D Energy Research Centre, School of Energy and Environment, City University of Hong Kong, Hong Kong, China

<sup>2</sup>Center of Nanomaterials for Renewable Energy (CNRE), State Key Lab of Electrical Insulation and Power Equipment, School of Electrical Engineering, Xi'an Jiaotong University, Xi'an 710049, China

<sup>3</sup>School of Automotive and Traffic Engineering, Jiangsu University of Technology, Changzhou, 213001, China

## ABSTRACT

In metal-air batteries, heteroatom-doped carbon catalysts have been widely regarded as promising substitutes for Pt-based catalysts for enhancing oxygen reduction reaction (ORR) performance owing to their excellent catalytic activity and low cost. Sulfur (S) is a potential heteroatom dopant. However, its large atomic radius causes limitations, such as edge-selective doping and low doping amount. Herein, we report a successful fabrication of edge-enriched S-doped carbon nanoflakes (ESCNs) with S doping amount as high as 6.04 at% by chemical vapor deposition (CVD) method using thiophene as carbon/sulfur source and basic magnesium carbonate (BMC) nanoflake as template. The as-obtained ESCNs are highly porous with well-crystallized graphite layers on the edge and possess a large specific surface area of  $1,306 \text{ m}^2 \text{ g}^{-1}$ , resulting in remarkable ORR catalytic performance under alkaline condition. The ORR yields a high current density of  $7.0 \text{ mA cm}^{-2}$  at  $-0.03 \text{ V}$  (vs. RHE) and outstanding durability. When applied in zinc-air batteries, the as-developed ESCNs demonstrate superior electrochemical performance under different discharge current densities.

**Keywords:** *Heteroatom doping; Chemical vapor deposition; Template synthesis; Edge exposure; Zinc-air battery*

\* Corresponding author. Tel.: +852-3442-4626; fax: +852-3442-0688

E-mail address: mkh.leung@cityu.edu.hk

## 1. INTRODUCTION

Oxygen reduction reaction (ORR), which is a fundamental reaction for electrochemical energy

storage and conversion, has been hindered by its sluggish kinetics for wide applications. Pt-based catalysts show prominent ORR catalytic activities, but suffer from high cost and scarcity [1]. Heteroatom (e.g. N, S and P)-doped carbon nanomaterials have been widely investigated as promising substitutes for Pt catalyst for decades due to low cost, superior catalytic activity and excellent durability [2]. Theoretical and experimental studies have shown that nitrogen (N)-doped carbon nanomaterials are excellent for ORR owing to the charge relocation induced by electronegativity difference between N and C [3].

Sulfur (S)-doped carbon can also deliver high ORR activities comparable to Pt by significant polarization in spin density, based on the first-principles investigations using density functional theory (DFT), from the aspect of reaction energy barrier [4]. However, the material fabrication is challenging due to its large atomic radius and high formation energy between sulfur and graphitic carbon [5,6]. Limited research has been done on S-doped carbon nanomaterials with highly porous structure for ORR [7]. Present related publications on S-doped carbon are about co-doping with other heteroatoms such as N, resulting either low S content or small specific surface area [8-10]. More research is essential.

In addition to heteroatom doping, edge/surface engineering is also of vital importance for enhancing ORR catalytic performance as the edge/surface atomic structures are unsaturated with large quantity of dangling bonds, which usually show high chemical reactivity and selectivity, greatly benefiting their applications in heterogeneous catalysis, energy conversion and storage [11]. Besides, S doping preferentially happens at the edge of carbon framework

Selection and peer-review under responsibility of the scientific committee of the 11th Int. Conf. on Applied Energy (ICAE2019).

Copyright © 2019 ICAE

due to the large atomic radius, thus edge-enriched nanostructures would result in a more efficient S doping and boost in ORR performance [12].

To date, there are two strategies for increasing edge/surface exposure of carbon nanomaterials. One is to directly exfoliate graphite layers via ball milling and plasma treatment, which usually require complex and expensive equipment or technologies. The other approach to enlarge the edge/surface area is to grow carbon nanostructures on template materials such as silica by chemical vapor deposition (CVD). Nevertheless, the removal of silica template demands etching in hazardous hydrofluoric acid. Ca- or Mg-based compounds, which are more economical, convenient and ecofriendly than silica, have been used to fabricate various carbon nanostructures for energy conversion and storage [13-15]. Particularly, by using basic magnesium carbonate (BMC) as template, Hu and co-workers developed carbon nanocages/N-doped carbon nanocages with benzene/pyridine acting as precursor, and these carbon nanostructures manifested superb performances in supercapacitors, ORR and lithium-sulfur batteries [16-18]. However, the BMC templating method has not been applied to fabrication of S-doped carbon nanostructures to the best of our knowledge.

Herein, we report a successful synthesis of edge-enriched S-doped carbon nanoflakes, namely ESCNs, via CVD approach using BMC-derived interconnected MgO nanoparticles and thiophene as templates and carbon/sulfur sources, respectively. Owing to the abundant edge area in hexagonal MgO template and the in-situ doping strategy, the ESCNs show a high S doping amount of 6.04 at% and a large specific surface area of  $1306 \text{ m}^2 \text{ g}^{-1}$  with desirable mesopores. As effective metal-free electrocatalysts, the ESCNs have demonstrated superior ORR properties in alkaline condition, exhibiting high catalytic activities ( $7.0 \text{ mA cm}^{-2}$  at  $-0.03 \text{ V}$  versus reversible hydrogen electrode (vs. RHE)) and outstanding durability. When applied in zinc-air batteries, the performance of the as-prepared ESCNs was excellent as ORR catalysts on the air cathode under different discharge current densities.

## 2. EXPERIMENTAL SECTION

### 2.1 Material Synthesis

In a typical synthesis, 2g basic magnesium carbonate ( $4\text{MgCO}_3 \cdot \text{Mg}(\text{OH})_2 \cdot 5\text{H}_2\text{O}$ , Alfa) was placed in an alumina ceramic crucible in a tube furnace. The temperature was then ramped up at a heating rate of  $10 \text{ }^\circ\text{C}/\text{min}$  under a constant Ar flow (200 sccm). When reaching a certain

target temperature (from 700 to  $1000 \text{ }^\circ\text{C}$ ), thiophene was introduced by the Ar flow for 30 min. After the CVD reaction, the furnace was naturally cooled down to room temperature under Ar flow. The ESCNs were obtained by immersing the intermediate products after CVD in concentrated hydrochloric acid, washing thoroughly with distilled water until the pH was neutral and finally drying at  $60 \text{ }^\circ\text{C}$  overnight. The resulting products were designated as ESCN700, ESCN800, ESCN900 and ESCN1000 according to the fabrication temperatures.

### 2.2 Material Characterization

X-ray diffraction (XRD) patterns were recorded using a Bruker D2 Phaser apparatus using Cu  $K\alpha$  radiation ( $\lambda=1.5418 \text{ \AA}$ ) operated at 30 kV and 10 mA. Transmission electron microscope (TEM), high-resolution TEM (HRTEM), high-angle annular dark-field scanning transmission electron microscopy (HAADF-STEM) and elemental mapping images were collected on a JEOL-2100 operated at 200 kV.  $\text{N}_2$  adsorption-desorption isotherms at  $-196 \text{ }^\circ\text{C}$  were performed on a Micromeritics ASAP 2020 analyzer.

### 2.3 Electrochemical Characterization

Electrochemical measurements were conducted in a conventional three-electrode system connected to a CHI 760 electrochemical work station (Shanghai Chenhua Apparatus Co. Ltd.). Glassy carbon electrode (GCE, 5 mm in diameter, PINE instruments, U.S.A.), Pt foil and Hg/HgO (1 M KOH) electrode were used as working, counter and reference electrodes, respectively. The homogeneous catalyst ink was prepared by ultrasonically dispersing 5.0 mg catalyst in a mixture of anhydrous ethanol (900  $\mu\text{L}$ ) and Nafion solution (0.5 wt%, 100  $\mu\text{L}$ ). A total amount of 12  $\mu\text{L}$  of ink was loaded for all the as-prepared catalysts and the benchmark Pt/C (20 wt%, PK Catalyst). All electrolytes were purged with high-purity  $\text{N}_2$  or  $\text{O}_2$  for 30 min before measurements.

In data analysis, the measured potentials vs. Hg/HgO were converted to the reversible hydrogen electrode (RHE) scale based on the Nernst equation. The electron transfer number were calculated according to Koutecky-Levich (K-L) equation.

For application in zinc-air batteries, the air cathode was prepared by spraying the catalyst ink, the same ink used in the electrochemical tests, onto a piece of carbon paper (P75T, Fuel Cell store). The mass loading was  $0.4 \text{ mg cm}^{-2}$  for both ESCN800 and commercial Pt/C. A polished Zn plate and 6 M KOH aqueous solution were used as the anode and the electrolyte, respectively.

### 3. RESULTS AND DISCUSSION

The microstructures of the as-prepared ESCNs were studied by TEM and HRTEM, revealing that ESCN800 exhibits well-defined carbon nanoflake morphology with distinct edges (Fig. 1a-c). Well-crystallized few-layer graphite structure is formed on the edge area, not only providing sufficient potential sites for sulfur doping but also excellent electric conductivity for catalyzing ORR. Furthermore, the nanoflakes of the ESCN800 are transparent and clear, indicating that they are quite thin and can facilitate the mass transport of oxygen-containing intermediates in ORR process, thus improve the ORR kinetics. Elemental mapping images (Fig. 1d) demonstrate the successful S doping and reveal uniform distribution of C, S and O atoms throughout the ESCN800.

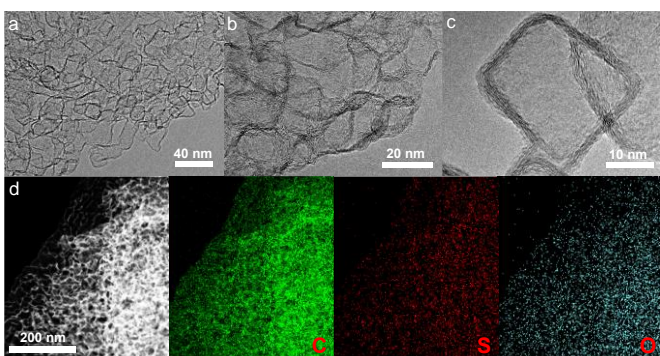


**Fig. 1.** Electron microscope images of ESCN800: (a-c) TEM images of ESCN800; (d) HAADF STEM image of ESCN800 with corresponding elemental mappings of C, S and O.

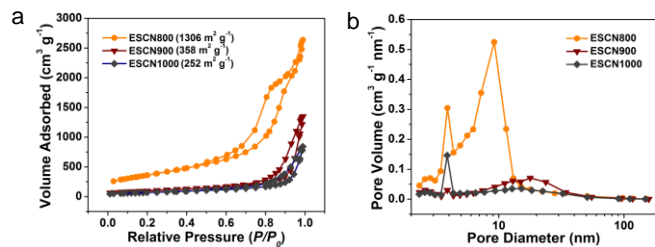


**Fig. 2.** N<sub>2</sub> adsorption-desorption isotherms of the ESCNs (a) and the corresponding pore size distributions (b).

Brunauer-Emmentt-Teller (BET) analysis shows that increasing the reaction temperature results in a decrease in the specific surface area, from 1,306 m<sup>2</sup> g<sup>-1</sup> for ESCN800 to 252 m<sup>2</sup> g<sup>-1</sup> for ESCN1000 (Fig. 2a). The presence of a slit and tilt hysteresis loop in the sorption isotherms of ESCN800 indicates a mixture type of ink bottle-neck pores and slit pores (H<sub>2</sub>+H<sub>3</sub> type based on IUPAC classification), which can be ascribed to the “cavities” and non-rigid aggregation resulting from the carbon nanoflakes, respectively [19,20]. The pore size evaluated from BJH desorption curve falls into a typical

mesoporous range with maximum distribution in 9.2 nm for ESCN800 (Fig. 2b).

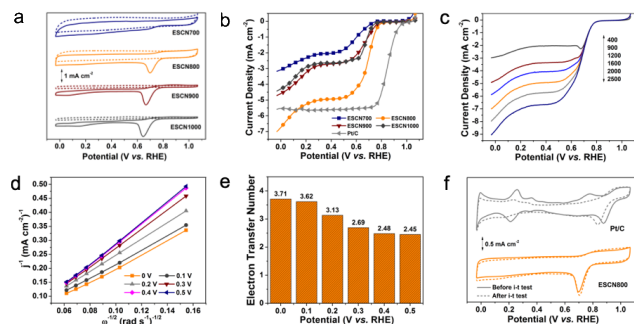


**Fig. 3.** ORR performances of the ESCNs in 0.1 M KOH: (a) CV curves of the ESCNs in N<sub>2</sub>- (dash) and O<sub>2</sub>-saturated (solid) conditions (scan rate: 10 mV s<sup>-1</sup>); (b) LSV curves of the ESCNs compared with commercial 20 wt% Pt/C (rotation speed: 1600 rpm, scan rate: 10 mV s<sup>-1</sup>); (c) LSV curves of ESCN800 at different rotation rates (scan rate: 10 mV s<sup>-1</sup>); (d) K-L plots of ESCN800 at various potentials; (e) Electron transfer number (n) of ESCN800 derived from K-L plots at various potentials; (f) Comparison of CV curves between ESCN800 and commercial 20 wt% Pt/C before and after i-t test at 0.47 V (vs. RHE) for 10 h (rotation speed: 1600 rpm, scan rate: 10 mV s<sup>-1</sup>).

The successful S doping, delicate edge-enriched flake-like morphology and large specific surface area of the as-fabricated ESCNs are greatly beneficial for ORR applications. The electrochemical performances of the ESCNs for ORR were investigated in detail under alkaline condition. Apart from no distinct ORR peak for ESCN700, cyclic voltammetry (CV) curves of ESCN800, ESCN900 and ESCN1000 exhibit remarkable oxygen reduction peaks in O<sub>2</sub>-saturated KOH solution (Fig. 3a). The ORR peak potential shifts negatively with increasing pyrolysis temperature from 800 to 1000 °C, suggesting an unfavorable influence of higher temperature to the catalytic activity of the ESCNs. Linear scanning voltammetry (LSV) curves of the ESCNs recorded by rotating disk electrode (RDE) follow the same trend (Fig. 3b). Although not as competitive as commercial Pt/C, the ESCN800 displays an onset potential of 0.81 V (vs. RHE), more positive than that of the other ESCNs. The current density of ESCN800 at -0.03 V (vs. RHE) reaches 7.0 mA cm<sup>-2</sup>, outperforming Pt/C and most reported S-doped carbon nanomaterials [21,22]. The remarkable ORR catalytic activities of ESCN800 can be ascribed to its unique nanostructure. The well-graphitized edges of the carbon nanoflakes lead to superior electric conductivity, and the extremely thin carbon nanoflakes are favorable for the electrolyte penetration and retention. Meanwhile, the large specific surface area of ESCN800

with abundant sulfur dopants provides plentiful of active sites for ORR.

To further explore the ORR kinetics on ESCN800, electron transfer number per oxygen molecule ( $n$ ) was calculated from the LSVs under different rotation rates according to K-L equation (Fig. 3c). The K-L plots of ESCN800 show good linearity between  $j^{-1}$  and  $\omega^{-1/2}$  (where  $j$  is the measured ORR current density and  $\omega$  is the rotation rate of RDE) from 0 V to 0.5 V (vs. RHE), indicating the first order reaction kinetics towards the concentration of the dissolves oxygen under alkaline condition (Fig. 3d) [23]. Based on the K-L plots, the  $n$  of ESCN800 for ORR is determined as 3.62 and 3.13 at 0.1 V and 0.2 V (vs. RHE), respectively, then reaches 3.71 at 0 V (vs. RHE). This shows that the ORR proceeds on the ESCN800 *via* a combination of two-electron and four-electron pathway at positive potentials, and then goes through a more efficient four-electron transfer mechanism when the potential is more negative than 0.1 V (vs. RHE) (Fig. 3e).

A comparison in ORR durability between ESCN800 and commercial Pt/C was also conducted in alkaline condition. The catalysts were subject to i-t test at 0.47 V (vs. RHE) for 10 h, and the CV curves of the ESCN800 and Pt/C before and after the i-t test were compared, respectively (Fig. 3f). It can be observed that the prominent ORR catalytic activities of ESCN800 are well maintained after 10 h i-t test in terms of onset potential, current density and electrochemical surface area (ESCA) which can be estimated by integration of the anodic-cathodic current densities at low potential range [24]. The slight increase in peak current density of the ESCN800 may result from the improved electrolyte infiltration during i-t test. In contract, the commercial Pt/C suffers from 44 mV negative-shift of onset potential and significant loss of ESCA over time due to aggregation and Ostwald ripening [25].

The excellent ORR performance of the ESCN800 implies great potential application as catalyst for metal-air battery cathode. To this end, we constructed primary Zn-air batteries with ESCN800 and Pt/C on Teflon-coated carbon paper as air cathode, respectively. The ESCN800-based Zn-air battery with open circuit voltage (OCV) as 1.36 V presents stable discharge curves at various discharge current densities (Fig. 4a). The output voltage can be maintained at 1.05 V in discharge at a current density of 10 mA cm<sup>-2</sup>.

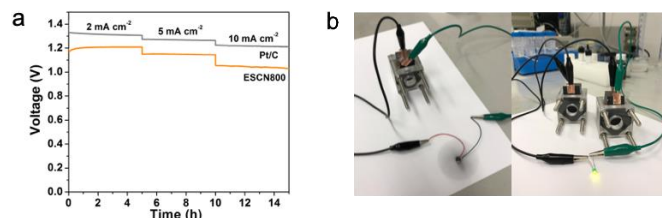


**Fig. 4.** Performance of primary Zn-air batteries: **(a)** Discharge curves of primary Zn-air batteries using ESCN800 and commercial 20 wt% Pt/C as ORR catalyst, respectively at various discharge current densities; **(b)** Fan (left) and LED (right) powered by Zn-air batteries.

#### 4. CONCLUSIONS

In summary, the ESCN800 with large specific surface area and high sulfur doping amount can be fabricated through CVD method using thiophene as carbon/sulfur source and basic magnesium carbonate (BMC) nanoflakes as template. The carbon growth with simultaneous S-doping has successfully addressed the challenge of low sulfur doping amount in carbon nanostructures via a combined templating-CVD synthesis strategy. Consequently, the ESCNs with thin graphitic layers and abundant active sites greatly contribute to the prominent ORR performance, surpassing that of the commercial Pt/C in terms of current density and durability. More importantly, the synthesis strategy of combining templating and CVD methods can be generally applied to fabricate various doped carbon nanostructures by choosing different carbon/dopant sources and templates. Besides, the material synthesis process is facile, cost-effective and high-yield; therefore, it has great potentials in energy related applications, such as fuel cell and metal-air battery.

#### ACKNOWLEDGMENTS

This work was supported by the Shenzhen Knowledge Innovation Program (Basic Research, JCYJ20160428154632404), the National Natural Science Foundation of China (NSFC) (21875200), the Natural Science Basis Research Plan in Shanxi Province of China (No. 2018JM5085), the Tang Scholar Program from the Cyrus Tang Foundation, and the Natural Science Foundation of Jiangsu Province (Grant No. BK20170314).

#### REFERENCES

- [1] Shao M, Chang Q, Dodelet J-P, Chenitz R. Recent Advances in Electrocatalysts for Oxygen Reduction Reaction. *Chem Rev* 2016;116:3594-7.
- [2] Antonietti M, Oschatz M. The Concept of “Noble, Heteroatom-Doped Carbons,” Their Directed Synthesis

by Electronic Band Control of Carbonization, and Applications in Catalysis and Energy Materials. *Adv Mater* 2018;30:1706836.

[3] Zhao Y, Wan J, Yao H, Zhang L, Lin K, Wang L, Yang N, Liu D, Song L, Zhu J, Gu L, Liu L, Zhao H, Li Y, Wang D. Few-layer graphdiyne doped with sp-hybridized nitrogen atoms at acetylenic sites for oxygen reduction electrocatalysis. *Nat Chem* 2018;10:924-31.

[4] Jeon I-Y, Zhang S, Zhang L, Choi H-J, Seo J-M, Xia Z, Dai L, Baek J-B. Edge-Selectively Sulfurized Graphene Nanoplatelets as Efficient Metal-Free Electrocatalysts for Oxygen Reduction Reaction: The Electron Spin Effect. *Adv Mater* 2013;25:6138-45.

[5] Kiciński W, Szala M, Bystrzejewski M. Sulfur-doped porous carbons: Synthesis and applications. *Carbon* 2014;68:1-32.

[6] Denis PA, Faccio R, Momburu AW. Is It Possible to Dope Single-Walled Carbon Nanotubes and Graphene with Sulfur? *ChemPhysChem* 2009;10:715-22.

[7] Bandosz TJ, Ren T-Z. Porous carbon modified with sulfur in energy related applications. *Carbon* 2017;118:561-77.

[8] Chen X, Chen X, Xu X, Yang Z, Liu Z, Zhang L, Xu X, Chen Y, Huang S. Sulfur-doped porous reduced graphene oxide hollow nanosphere frameworks as metal-free electrocatalysts for oxygen reduction reaction and as supercapacitor electrode materials. *Nanoscale* 2014;6:13740-47.

[9] Klingele M, Pham C, Vuyyuru KR, Britton B, Holdcroft S, Fischer A, Thiele S. Sulfur doped reduced graphene oxide as metal-free catalyst for the oxygen reduction reaction in anion and proton exchange fuel cells. *Electrochem Commun* 2017;77:71-5.

[10] Paraknowitsch JP, Thomas A. Doping carbons beyond nitrogen: an overview of advanced heteroatom doped carbons with boron, sulphur and phosphorus for energy applications. *Energy Environ Sci* 2013;6:2839-55.

[11] Tang C, Zhang Q. Nanocarbon for Oxygen Reduction Electrocatalysis: Dopants, Edges, and Defects. *Adv Mater* 2017;29:1604103.

[12] Zhang L, Niu J, Li M, Xia Z. Catalytic Mechanisms of Sulfur-Doped Graphene as Efficient Oxygen Reduction Reaction Catalysts for Fuel Cells. *J Phys Chem C* 2014;118:3545-53.

[13] Wang H, Wang J, Cao D, Gu H, Li B, Lu X, Han X, Rogach AL, Niu C. Honeycomb-like carbon nanoflakes as a host for SnO<sub>2</sub> nanoparticles allowing enhanced lithium storage performance. *J Mater Chem A* 2017;5:6817-24.

[14] Gu H, Cao D, Wang J, Lu X, Li Z, Niu C, Wang H. Micro-CaCO<sub>3</sub> conformal template synthesis of hierarchical

porous carbon bricks: As a host for SnO<sub>2</sub> nanoparticles with superior lithium storage performance. *Mater. Today Energy* 2017;4:75-80.

[15] Cao D, Dai Y, Xie S, Wang H, Niu C. Pyrolytic synthesis of MoO<sub>3</sub> nanoplates within foam-like carbon nanoflakes for enhanced lithium ion storage. *J Colloid Interface Sci* 2018;514:686-93.

[16] Chen S, Bi J, Zhao Y, Yang L, Zhang C, Ma Y, Wu Q, Wang X, Hu Z. Nitrogen-Doped Carbon Nanocages as Efficient Metal-Free Electrocatalysts for Oxygen Reduction Reaction. *Adv Mater* 2012;24:5593-7.

[17] Xie K, Qin X, Wang X, Wang Y, Tao H, Wu Q, Yang L, Hu Z. Carbon Nanocages as Supercapacitor Electrode Materials. *Adv Mater* 2012;24:347-52.

[18] Lyu Z, Xu D, Yang L, Che R, Feng R, Zhao J, Li Y, Wu Q, Wang X, Hu Z. Hierarchical carbon nanocages confining high-loading sulfur for high-rate lithium-sulfur batteries. *Nano Energy* 2015;12:657-65.

[19] Nayak NB, Nayak BB. Temperature-mediated phase transformation, pore geometry and pore hysteresis transformation of borohydride derived in-born porous zirconium hydroxide nanopowders. *Sci Rep* 2016;6:26404.

[20] AlOthman ZA. A Review: Fundamental Aspects of Silicate Mesoporous Materials. *Materials* 2012;5:2874-902.

[21] El-Sawy AM, Mosa IM, Su D, Guild CJ, Khalid S, Joesten R, Rusling JF, Suib SL. Controlling the Active Sites of Sulfur-Doped Carbon Nanotube-Graphene Nanolobes for Highly Efficient Oxygen Evolution and Reduction Catalysis. *Adv Energy Mater* 2016;6:1501966.

[22] Li W, Yang D, Chen H, Gao Y, Li H. Sulfur-doped carbon nanotubes as catalysts for the oxygen reduction reaction in alkaline medium. *Electrochim Acta* 2015;165:191-7.

[23] She Y, Chen J, Zhang C, Lu Z, Ni M, Sit PHL, Leung MKH. Nitrogen-doped graphene derived from ionic liquid as metal-free catalyst for oxygen reduction reaction and its mechanisms. *Appl Energy* 2018;225:513-21.

[24] Sheng W, Myint M, Chen JG, Yan Y. Correlating the hydrogen evolution reaction activity in alkaline electrolytes with the hydrogen binding energy on monometallic surfaces. *Energy Environ Sci* 2013;6:1509-12.

[25] Chen S, Wei Z, Qi X, Dong L, Guo Y-G, Wan L, Shao Z, Li L. Nanostructured Polyaniline-Decorated Pt/C@PANI Core-Shell Catalyst with Enhanced Durability and Activity. *J Am Chem Soc* 2012;134:13252-5.